Journal of Biomedical Optics

SPIEDigitalLibrary.org/jbo

Multiplexed living cells stained with quantum dot bioprobes for multiplexed detection of single-cell array

Dahai Ren
Yiqiu Xia
Zheng You

SPIE

Multiplexed living cells stained with quantum dot bioprobes for multiplexed detection of single-cell array

Dahai Ren, Yiqiu Xia, and Zheng You
Tsinghua University, Department of Precision Instrument, State Key Laboratory of Precision Measurement Technology and Instruments, Beijing 100084, China

Abstract. The results of quantum dot (QD) probe preparation for multiplexed single-cell array staining and analysis are reported. By controlling the reaction temperature, time, and ratio of Cd to Se, multicolor CdSe QDs emitting fluorescence ranging from purple to red in a safer, simpler, and more convenient way than traditional methods is obtained. To detect cells using these oil-soluble QDs, they are first coated with water-soluble thioglycolic aid (TGA) so that biocompatible multiwavelength bioprobes can be obtained. QDs' surface is somewhat damaged when binding TGA to QDs is found, which results in a reduction of QDs' emission wavelength and a slight blue shift of QDs' emission wavelength after water-soluble modification with TGA. Comparison of the emission spectrum showed that it is negligible, and the fluorescent properties of QDs capped by TGA are still satisfactory. Living cells are then stained with multiplexed probes by conjugating TGA-QDs with antibodies specific to these cell antigens. Changes in fluorescence intensity can indicate change in the relative quantity of antigens expressed in the same cell caused by external stimulus, offering effective methods to multiplexed optical analysis of single cells. [DOI: 10.1117/1.JBO.18.9.096005]

Keywords: quantum dots; fluorescence spectrum; bioprobe; multiplexed staining; bio-MEMS.

Paper 130181R received Mar. 28, 2013; revised manuscript received May 31, 2013; accepted for publication Aug. 7, 2013; published online Sep. 3, 2013.

1 Introduction

The potential application of quantum dots (QDs) as bioprobes is promising due to their quantum scale effects and special fluorescent properties. When compared with normal fluorescent materials, QDs have advantages including long-term photostability, higher intensity, tunable size, broad UV excitation profiles, and narrower emission spectra.[1,2] These properties allow QDs to label different materials at the same time,[3,4] contributing to their usefulness as qualitative and quantitative probes for multiplexed detection.[5–7] QDs provide new approaches for real-time, high-sensitivity, and dynamic fluorescent imaging in DNA and protein detection as well as relevant biochips and biosensors.[8–10] Tumors have cellular heterogeneity, which leads to different responses to drugs and the environment as well as the failure of cancer treatment.[11,12] Therefore, it is important to study cancer cells' cellular heterogeneity. With the single-cell array, we can micropattern cells as designed; so, we can focus on the individual behaviors and their reactions to the drugs, rather than that of the cell colony. As a result, we can have a better understanding of cellular heterogeneity. Combining single-cell arrays with QD probes, we can achieve multiplexed detection of the behaviors of individual cells and high-throughput drug screening.

CdE (E is S, Se, or Te) QDs have high quantum yield, good fluorescence properties, and long-term fluorescence stability and can easily be modified as bioprobes for biomedical detections. In the late 1980s and early 1990s, Stuczynski et al.[13] and Murray et al.[14] obtained CdE QDs using an organic system $Cd(CH_3)_2$. Although Bowen et al.,[15] Peng et al.,[16] and Peng et al.[17] improved the method, it still requires difficult experimental conditions and is susceptible to explosion. In 2001, Peng and Peng[18] obtained high-quality CdE QDs and avoided a latent explosion by using CdO instead of $Cd(CH_3)_2$. Unfortunately, octadecene (ODE) solvents and organic ligand trioctylphosphine oxide (TOPO) are expensive and poisonous, which makes this method impractical. In 2005, Deng et al.[19] replaced ODE and TOPO with paraffin liquid and oleic acid (OA), developing a low-cost and environment-friendly approach to prepare CdSe QDs. This approach allows easier control of the diameter of QDs and reduces their nucleation rate.

Besides CdE QDs, other QDs like ZnS QDs, ZnO QDs, and carbon nanoparticals are also used as new quantum fluorescent materials in cell imaging and drug studies. Although ZnO QDs have relatively poorer characteristics of quantum yield and water solubility than CdE QDs, they have advantages of nontoxic, low cost, and long-term fluorescence stability. This allows their extensive application in biomedical research.[20–22] In 2010, Yuan et al.[23] synthesized water-dispersed ZnO QDs and successfully loaded them with anticancer drugs to deliver them. In 2012, Jia and Misra[24] immobilized many ZnO QDs on a silica nanosphere increasing its quantum yield and photoluminescence in bioimaging. In addition, silica nanospheres offered good water compatibility and chemical stability.

Although QDs synthesized in organic systems have better spectral properties than those synthesized in water, hydrophilic modification is still required because of their fat-soluble characteristics when used as bioprobes. These fat-soluble QDs are usually modified by sulfhydryl compounds,[25,26] silanization,[27,28] microspheres,[29,30] and electrostatic interaction.[31]

Address all correspondence to: Dahai Ren, Tsinghua University, Department of Precision Instrument, State Key Laboratory of Precision Measurement Technology and Instruments, Beijing 100084, China. E-mail: rendh@tsinghua.edu.cn

QDs have advantages in real-time dynamic fluorescent analysis, because they are sensitive and simple to be used in image acquisition. Here, we focused on the QDs' unique fluorescent characteristics to realize their usefulness in multiplexed staining of cells. To obtain probes of a broader fluorescence range for multiplexed staining in an easier, lower-cost, and more environment-friendly way, paraffin liquid was used as solvent and OA as stabilizer. The relationships between QD's emitting wavelengths and several synthesizing conditions are investigated in detail including temperature, time, and ratio of Cd to Se. By controlling the reaction temperature, time, and ratio of Cd to Se, we obtained stable multicolor QDs emitting fluorescence ranging from purple to red with a lower temperature and a shorter time, which is much safer, simpler, and more convenient than traditional methods.

To detect cells using these lipid-soluble QDs, they were capped with thioglycolic aid (TGA), which allowed the synthesis of water-soluble and biocompatible multiwavelength bioprobes. Furthermore, we stained living cells with multiplexed probes by conjugating TGA-QDs with antibodies and by using specific binding between the antibodies and the antigens. With the media of antibodies, we can study antigens with QD probes. Detecting QDs' fluorescence can indicate the relative quantity of the antigens expressed by a single cell, which allows the multiplexed detection of a single-cell array. The relative quantity of antigens expressed by the same cell can be shown by analyzing changes in the fluorescence of a single cell in reaction with drug stimuli or environmental variation. With the same method, we can also label other targets (such as protein, peptides, biotinylated materials, and chemicals with amidogen) to study the behaviors of cells. These qualities of QDs meet the requirements for their use in multiplexed optical analysis of single-cell arrays, which is difficult in most cases at present.

2 Materials and Methods

2.1 *Materials*

Cadmium oxide (CdO), Selenium (Se) powder, OA (analytical grade), paraffin liquid (analytical grade), cyclohexane (analytical grade), TGA (analytical grade), methyl alcohol (analytical grade), 1-ethyl-3-(3-dimethylaminopropyl)carbodiimide (EDC) (analytical grade), and phosphate buffer solution (PBS) (pH = 7.2 to 7.4) were used.

2.2 *Synthesis of CdSe QDs*

To prepare stock Cd solution, a mixture of CdO (1.284 g, 10 mmol), OA (10 mL), and paraffin liquid (20 mL) are loaded into a three-neck flask. Next, the mixture is heated slowly to 150°C in nitrogen. The heating process continues at 150°C until all CdO dissolves, generating a dark red homogeneous Cd solution. To prepare the stock Se solution, we loaded Se powder (0.04 g, 0.5 mmol) and paraffin liquid (30 mL) in another three-neck flask and heated the mixture slowly to 210°C in nitrogen. The heating process continued at 220°C with rapid stirring until all Se powder dissolved, generating a yellow homogeneous Se solution. Then, we injected the Cd stock solution (3 mL, containing 1 mmol Cd) into the Se stock solution (Cd:Se = 2:1) and kept the mixture reacting at 220°C to grow the CdSe QDs. Finally, the QDs are separated by centrifugation, wash the QD deposit several times using cyclohexane and airproof them in cyclohexane at 4°C.

2.3 *Water-Soluble Modification of QDs*

First, we extracted 1 mL of the QDs solution and diluted it using 2 mL cyclohexane. Once diluted, we added 0.25 mL TGA to the QD and cyclohexane solution, and TGA-QDs (Fig. 1) floccules were obtained by concussing the mixture for 30 min. Next, the solution was centrifuged at 5000 rpm to remove the supernatant, and TGA-QDs deposition was extracted. The TGA-QDs deposition was further purified after washing three times with methyl alcohol. After washing with methyl alcohol, the homogeneous TGA-QDs aqueous solution was made by dissolving TGA-QDs in PBS. Finally, the solution was washed at least three times with PBS. During this process, a 100,000 MWCO membrane spin filter was used to remove large aggregates.

2.4 *Conjugating Antibodies with TGA-QDs*

To conjugate TGA-QDs with antibodies, we diluted TGA-QDs (QD620: red and QD520: green) with 600 μL PBS and mixed the solution with EDC and antibodies (anti-human CD15 and anti-human CD45). The mixing ratios used were TGA-QDs:EDC:antibodies = 1:1000:0.5 (mol). Next, the solution was incubated at 25°C by shaking 2 h in the dark and by blocking the reaction at 4°C overnight. This allows the unreacted EDC to hydrolyze and to lose its activity. Finally, the solution is washed at least three times with PBS. During this process, a 10,000 MWCO membrane spin filter is used to remove unconjugated TGA-QDs, after which the QD-antibody solution is obtained (Fig. 2).

2.5 *Single Staining and Multiplexed Staining with QDs*

The human promyelocytic leukemia cell-line HL60 was maintained in Roswell Park Memorial Institute (RPMI-1640) medium with 10% fetal bovine serum and 1% penicillin–streptomycin solution. The cells were cultured in humidified atmosphere at 37°C and 5% CO_2.

Li and Ho proposed an approach for cells patterning by generating a two-dimensional hexamethyldisilazane monolayer on the glass substrates, a protein adsorption template.[32] Also, we have reported a cells patterning result of human promyelocytic

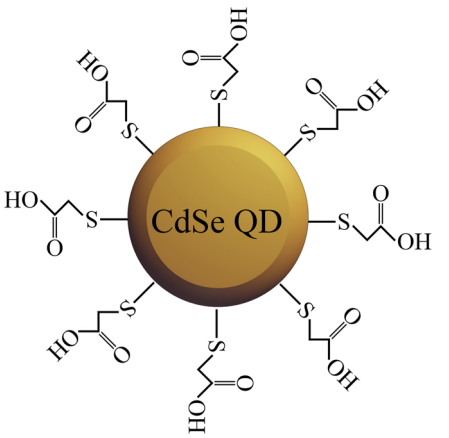

Fig. 1 Schematic diagram of a thioglycolic aid (TGA)-capped CdSe quantum dot (QD).

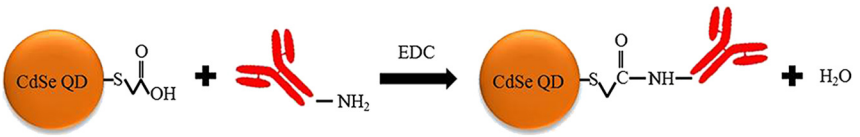

Fig. 2 Schematic diagram of conjugating QD with antibody.

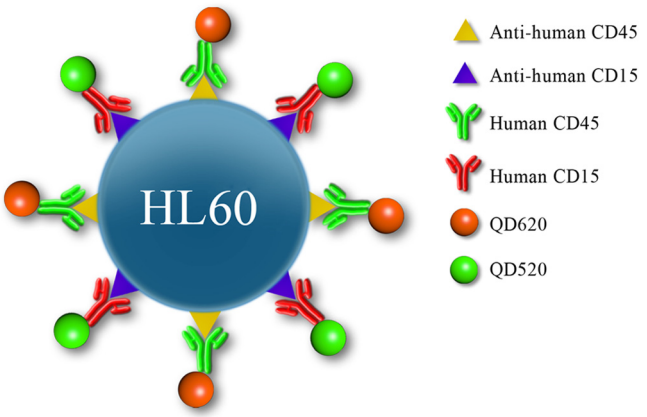

Fig. 3 Schematic diagram of multiplexed-stained cell HL60.

leukemia cells based on bio-MEMS.[33] In single-cell staining, cells were incubated with QD-antibodies (conjugation of QD620 and anti-human CD45) for 1 h. Next, cells were washed three times with PBS to remove unstained QD-antibodies. For multiplexed staining, we prepared two types of QD-antibody conjugates, QD520 with anti-human CD15,[34,35] and QD620 with anti-human CD45.[36,37] Using the same method as described above, cells were incubated using a mixture of QD520–anti-human CD15 and QD620–anti-human CD45 for 1 h. Finally, the cells were washed three times with PBS to remove unstained conjugates (Fig. 3).

2.6 *Spectral Imaging and Signal Quantitation*

An Olympus IX71 fluorescence microscope was employed to capture images with exciter filter BP470-495 and barrier filter BA510-IF. The exposure time was 200 ms, and the magnifications were 100× and 200×, based on which the intensity maps of multiple spectral distributions were calculated, as described above.

3 Results and Discussion

3.1 *Influences of Reaction Time and Temperature on QD Properties*

During synthesis, the reaction time determines the growth time of QDs sequentially affecting the diameters of QDs. To study this influence, we synthesized QDs at 220°C (when Cd:Se = 2:1) and extracted samples of the solution at 15 s, 30 s, 1 min, 5 min, 10 min, 30 min, and 1 h time points. Next, we diluted and cooled the solution in cyclohexane, obtaining QDs at different time points. We also observed the fluorescence of the washed and dried QDs under the UV light. As the reaction time increases, the QDs' fluorescence changed from purple to orange.

We also measured the emission spectrum of QDs that have reacted for 1 min, 5 min, 10 min, 30 min, and 1 h (sample nos., respectively: I-1, I-2, I-3, I-4, and I-5). From this spectrum, we observed a red shift (Fig. 4) with a wavelength ranging from 537.5 to 596.5 nm (Table 1). Since QDs grow as time goes by, their diameters became bigger for which the fluorescence generates a red shift. However, the rate of QDs' growth slows as time goes by, so does the speed of fluorescence's red shift.

To broaden the range of QDs' fluorescence, we took the influence of the reaction temperature into consideration. Instead of synthesizing QDs at 220°C, we increased the synthesizing temperature to 250°C. Under this temperature, we can see obvious red shift of QDs' fluorescence as the temperature increases under UV light without using complex equipment. Meanwhile, risks that often occur at higher temperatures can also be avoided. Moreover, we compared QDs' emission spectrum synthesized at 220°C and 250°C to learn the specific trend and the increasing rate of QDs' emission wavelength with the temperature. Based on these results, we can obtain specific synthesizing parameters when preparing QDs probes of certain fluorescence for the analysis of single-cell array. We extracted part of the solution with the same reaction time above (sample nos.: II-1, II-2, II-3, II-4, and II-5) and compared the fluorescence wavelength of QDs growing at 220°C with those growing at 250°C (Table 1).

Table 1 shows that emitting wavelengths of QDs at 250°C are longer than those at 220°C with the same growth rate, and after reacting for 1 h, we obtain QDs which emit red lights under the UV light (Fig. 5). It is, therefore, concluded that the growth speed of QDs increases as temperature rises. As a result, the diameter of QDs synthesized with the same duration at a higher temperature increases, leading to a red shift in the fluorescence. Therefore, we can obtain QDs of long-wavelength fluorescence

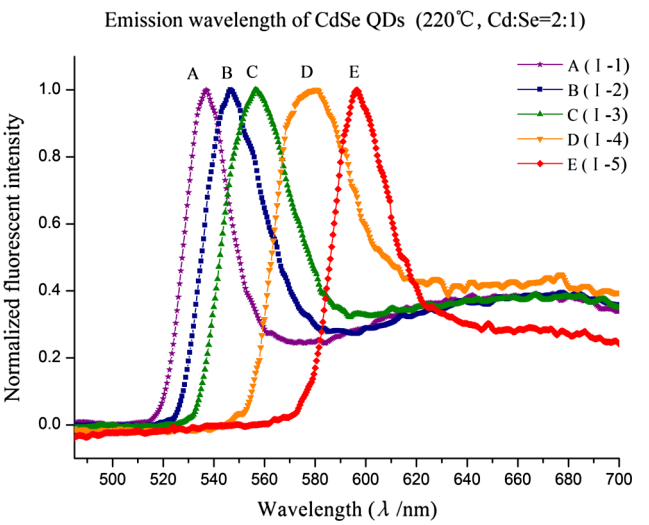

Fig. 4 Influence of reaction time on emission spectrum of QDs (220°C, Cd:Se = 2:1) (normalized image).

Table 1 Wavelength of quantum dots (QDs) (Cd:Se = 2:1) with varied reaction temperature and time.

Reaction temperature	Emission wavelength (λ/nm) with varied reaction time				
	1 min	5 min	10 min	30 min	60 min
220°C	537.5 nm	546.5 nm	556.5 nm	580.5 nm	596.5 nm
250°C	544.5 nm	553.5 nm	560.5 nm	593.5 nm	608.5 nm

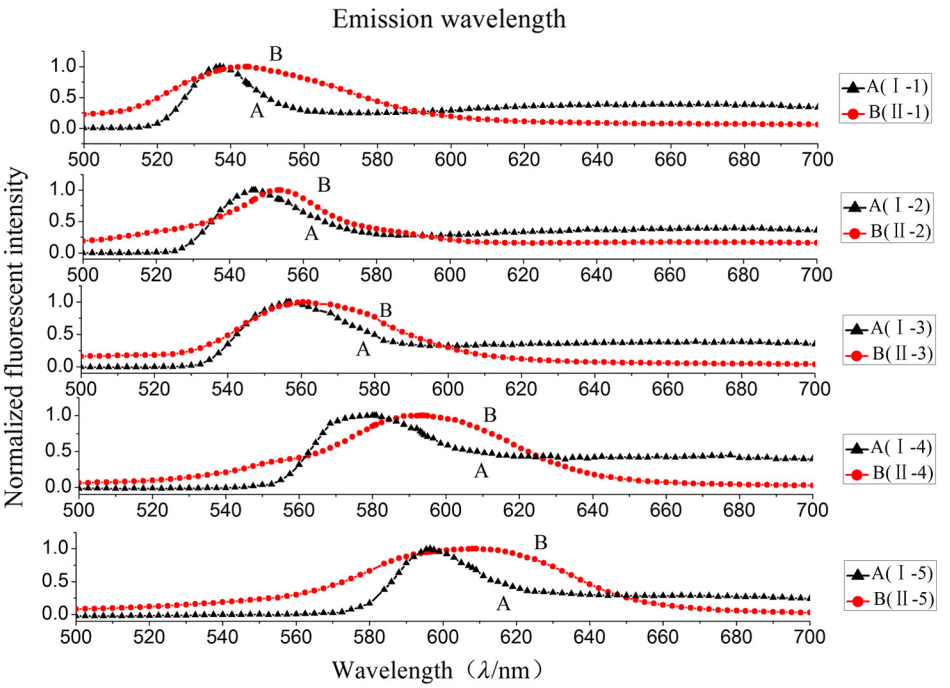

Fig. 5 Influence of temperature on emission spectrum of QDs (Cd:Se = 2:1; 220°C and 250°C) with varied reaction time (normalized image).

by enhancing the reaction temperature with the same reaction time.

As discussed above, since the speed of QDs' growth is slower at lower temperatures, the wavelength of the fluorescence is also shorter. On the contrary, the wavelength of fluorescence is longer at higher temperatures. Therefore, by combining these two reaction temperatures, we can obtain QDs with various fluorescence, meeting the requirement of multicolor QDs for the multiplexed detection of the single-cell array.

3.2 *Influence of Ratio of Cd to Se on Properties of QDs Synthesized*

Although the fluorescence of QDs will generate a red shift when the temperature increases, the speed of QDs' growth using this method is generally slow. Therefore, it takes a long time to gain QDs that emit fluorescence of long wavelength with the speed of QDs' growth becoming slower as the reaction continues. Unless QDs are incubated at a high temperature, it is difficult to obtain long wavelength fluorescence such as red.

To reduce the reaction time, we can further increase the temperature; but this increases the difficulty and the risk of the experiment, while negatively affecting the control of the QD diameter. In order to shorten the reaction time, while maintaining the simplicity and safety of the experiment, we should take other factors into consideration like the ratio of Cd to Se.

When increasing the ratio from 2 to 6, we can see a red shift in QDs' fluorescence. To learn the specific trend and the increasing rate of QDs' emission wavelength as guidance for synthesizing QDs probes of a certain fluorescence, we also compared the emission spectrum of QDs synthesized at the ratios of Cd to Se at 2 and 6 and the reaction temperature of 220°C. When the reaction times are 1 min, 5 min, 10 min, 30 min, and 1 h (sample no. with ratio 6, respectively: III-1, III-2, III-3, III-4, and III-5), we extracted samples of the reaction solution to obtain QDs and compared their emission wavelength (Table 2).

Table 2 shows a red shift of the fluorescence as a result of the acceleration of QDs' growth (Fig. 6) when the ratio of Cd to Se increases with the same reaction time and temperature. Therefore, we can obtain longer emission wavelength QDs in a shorter time, as long as the ratio of Cd to Se increases. Particularly, we can obtain red fluorescence (629.0 nm) when the ratio is 6, rather than orange fluorescence (596.5 nm) when the ratio is 2, using the same reaction time (60 min). In conclusion, we can effectively shorten the reaction time to synthesize long emission wavelength QDs by controlling the ratio of Cd to Se.

Table 2 Wavelength of QDs (220°C) with different ratio of Cd to Se and different reaction time.

Ratio of Cd to Se	Emission wavelength (λ/nm) with different reaction time				
	1 min	5 min	10 min	30 min	60 min
2	537.5 nm	546.5 nm	556.5 nm	580.5 nm	596.5 nm
6	535.5 nm	571.5 nm	583.5 nm	619.0 nm	629.0 nm

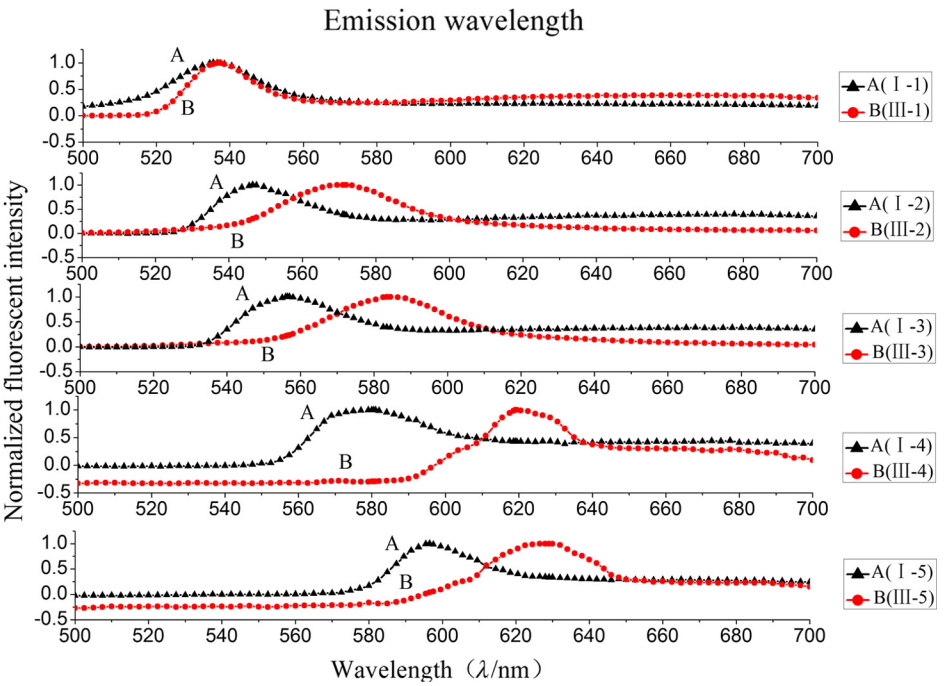

Fig. 6 Influence of ratio on the emission spectrum of QDs (220°C, the ratios of Cd to Se are 2 and 4, respectively) with varied reaction time (normalized image).

The red shift of QD fluorescence can be achieved more effectively by increasing the ratio from 2 to 6, which is also safer and easier when compared with raising the reaction temperature from 220℃ to 250℃. In order to broaden the range of QDs' emission wavelength to the maximum extent for multiplexed detection, this ratio is given priority in the following experiments.

Based on the influence of the reaction time, ratio of Cd to Se, and temperature on fluorescent properties of CdSe QDs, we can effectively obtain multicolor QDs with fluorescence varying from purple to red in a short reaction time meeting the requirements for a multiplexed cell assay and improving the capacity of the assay with a broad color range.

What is more, with the specific parameters of the reaction time, the temperature, and the ratio, we can synthesize the QDs of suitable fluorescent wavelength with a lower temperature and shorter time, which is safer, simpler, and more convenient in most cases.

3.3 *Characterization of QDs' Water-Soluble Modification*

In order to test the effect of water-soluble modification by TGA, we capped TGA to QDs solution I-3, II-4 and III-4, respectively [sample no.: I-3 (TGA), II-4 (TGA), and III-4 (TGA)] and detected their emission spectrum (Table 3).

By comparing the emission spectrum (Fig. 7), we can find that after water-soluble modification with TGA, a slight blue shift of QDs' emission wavelength occurred. When binding TGA to QDs, QDs' surface is somewhat damaged resulting in a reduction in QDs' emission wavelength. However, the blue shift caused by this modification is negligible, and the fluorescent properties of QDs capped by TGA are still satisfactory. Therefore, water-soluble modified QDs of various emission wavelengths can be employed for multiplexed labeling,

Table 3 Emission wavelengths of QDs before and after water-soluble modification.

Sample no.	I-3	II-4	III-4
Wavelength before modification	556.5 nm	619.0 nm	593.5 nm
Wavelength after modification	548.5 nm	601.0 nm	590.0 nm

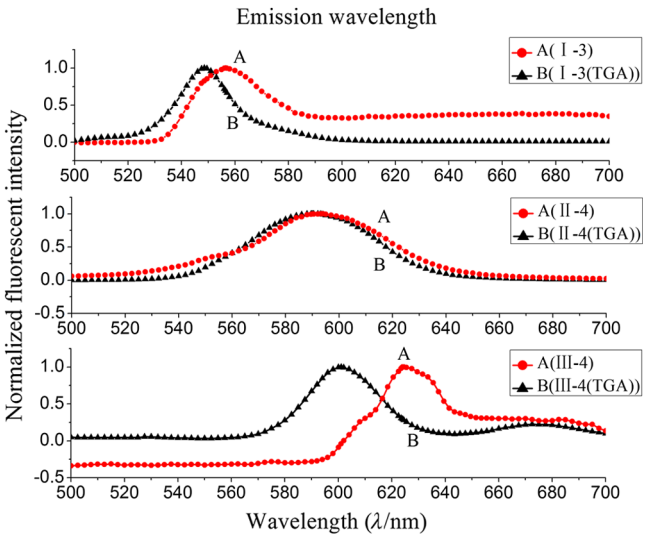

Fig. 7 Influence of water-soluble modification on emission spectrum of QDs (normalized image).

which can easily be distinguished under the fluorescence microscope.

3.4 *Conjugating Antibodies with TGA-QDs*

When studying cells' behaviors or reactions to drugs, it is important to detect their abilities to express proteins or transmit signals. As it is difficult to conjugate proteins expressed by cells inside or on the surface with QD probes, we can conjugate QDs with these proteins' antibodies. This allows the labeling of target proteins, by which we can study the behaviors of these proteins with QD probes. Moreover, when detecting cancer cells, we also utilize fluorescence in labeled antibodies to conjugate with cancer markers. In the following studies, we utilize QDs to conjugate antibodies and staining cells, so that we can study the labeling and staining characteristics of QD probes. With the same method, we can also conjugate QDs with other targets, like proteins and peptides, to study cell behaviors.

With catalysis of EDC, the carboxyl of TGA and the amino residue of the antibodies can become amide linkage combining TGA-QDs and antibody. In order to confirm whether antibodies were conjugated with TGA-QD, we first conjugated QD620 with anti-human CD45 (molecular weight: 150 kD), using the method described above. The different components of the mixture were then separated using SDS-PAGE electrophoresis (Fig. 8).[38] In channel 1, the solution was washed with a 100,000 MWCO membrane spin filter to remove unconjugated QDs. In channel 2, the solution was unchanged.

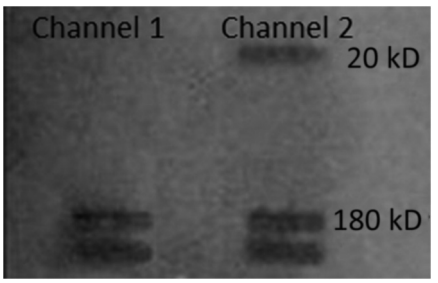

Fig. 8 The image of SDS-PAGE electrophoresis. Channel 1 is the result after washed by ultrafiltration to remove unconjugated QDs. Channel 2 is the original result.

From the image of the SDS-PAGE gel electrophoresis, we can see that there are three bands—QD620, anti-human CD45, and QD620–anti-human CD45, respectively, in channel 2. In channel 1, as QDs were removed by ultrafiltration, there are only two bands, whose molecular weights are the same as the components in the channel 2. Since we can find the bands of QD620–anti-human CD45 in the image of the gel electrophoresis, we can conclude that we can obtain QDs-conjugated antibodies using the method mentioned above, which can be used as bioprobes. However, we can still find unconjugated antibodies in the washed solution, as shown on the image of channel 1. In order to minimize the quantity of unconjugated antibodies to alleviate the interference on cell staining, we make TGA-QDs excessive in amount when conjugating.

3.5 *Single Staining with QDs*

QDs have long-term photostability and fluorescent intensity. They are about 100 times as stable as rhodamine 6G (R 6G) against photobleaching (QDs' time constant $t_{1/2} = 960$ s, R 6Gs' time constant $t_{1/2} = 10$ s) and about 20 times as strong as R 6Gs' fluorescence intensity.[39] Therefore, we can use QDs for long-term tracing and do not need to consider the changes in fluorescent intensity of individual QD probes when calculating the relative quantity of the targets through analyzing QD probes fluorescent intensity.

Utilizing the QD bioprobe preparation method as described above, we conjugated QD620 with anti-human CD45 to obtain QD620–anti-human CD45 and stained living HL60 cells with QD620 probes (red). Comparing the fluorescent image [Fig. 9(a1)] with the bright-field image [Fig. 9(a2)] at 100× magnification, we can find that the cells were dyed red, leading to cells' single staining with QDs successfully. With 200× magnification [Figs. 9(b1) and 9(b2)], we can find that most of the cells have been dyed red, yet the intensity of the fluorescence is different. The intensity of the fluorescence is determined by the human CD45's expression of the cell; the more the antigens on the cell, the stronger the fluorescence. From the fluorescent images of the stained cells, we can conclude that QD-antibodies prepared by the above-mentioned methods are suitable bioprobes for single-cell array. Changes in fluorescence intensity can indicate the dynamic antigens' expression in the same cell. Moreover, with the long-term photostability of QDs, we can continuously trace fluorescent changes of the cells for a long time to study these antigens' behaviors when stimulated by chemicals or environmental changes.

3.6 *Multiplexed Staining with QDs*

As QDs have a broad excitation spectrum, we can excite most of the QDs with different fluorescence under the same light source at the same time. We can also detect more than one targets labeled by different QD probes at the same time without switching among different exciting lights.

To carry out multiplex detection of single-cell array, we should investigate whether QD-antibodies could be employed as multiplex probes and multiplexed staining of the cells could be accomplished. By conjugating QD520 to anti-human CD15 and QD620 to anti-human CD45, we obtained two types of bioprobes: QD520–anti-human CD15 (green) and QD620–anti-human CD45 (red). With these two probes,

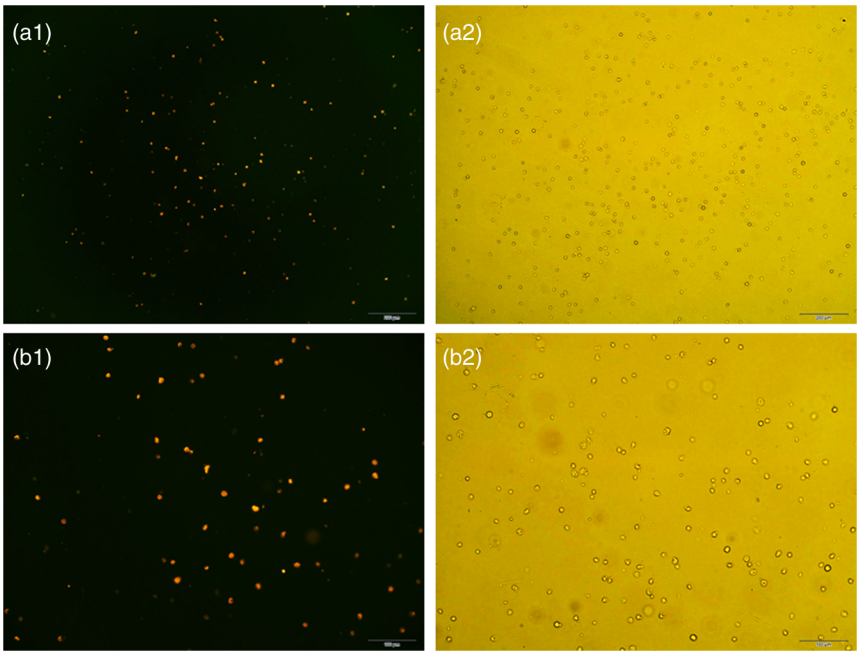

Fig. 9 The image of single-stained cells (QD620: red). (a1) The fluorescence image. (a2) The bright-field image, 100×, bar: 200 μm. (b1) The fluorescence image. (b2) The bright-field image, 200×, bar: 100 μm.

we multiplexed stained living HL60 cells. By comparing the fluorescence image [Fig. 10(a1)] and the bright-field image [Fig. 10(a2)] at 100× magnification, we can find that most of the cells have been stained by three main fluorescence: red, yellow, and green. With 200× magnification [Figs. 10(b1) and 10(b2)], we can find that cells have various fluorescence from green to red. When the red and green fluorescence are mixed, the observed fluorescence becomes yellow; and the color of the mixed fluorescence deepens as the red fluorescence increases and vice versa. By analyzing the fluorescence of the cells, we can obtain the relative quantity of antigens expressed. The redder the cells, the more the human CD45 is expressed by the cells and vice versa. Therefore, from the fluorescence images of the cells, we can conclude that these QD-antibodies are also appropriate probes for multiplexed staining. This type of fluorescence can also indicate changes in the relative quantity of different antigens expressed by the same single cell caused by external stimuli. Moreover, we can also trace more than

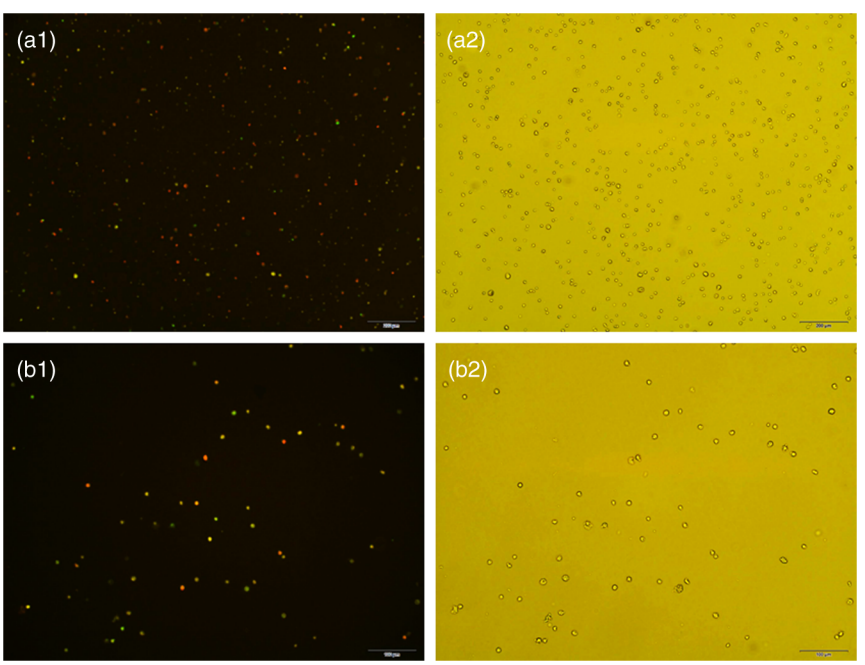

Fig. 10 The image of multiplexed-stained cells (QD620: red and QD520: green). (a1) The fluorescent image. (a2) The bright-field image, 100×, bar: 200 μm. (b1) The fluorescent image. (b2) The bright-field image, 200×, bar: 100 μm.

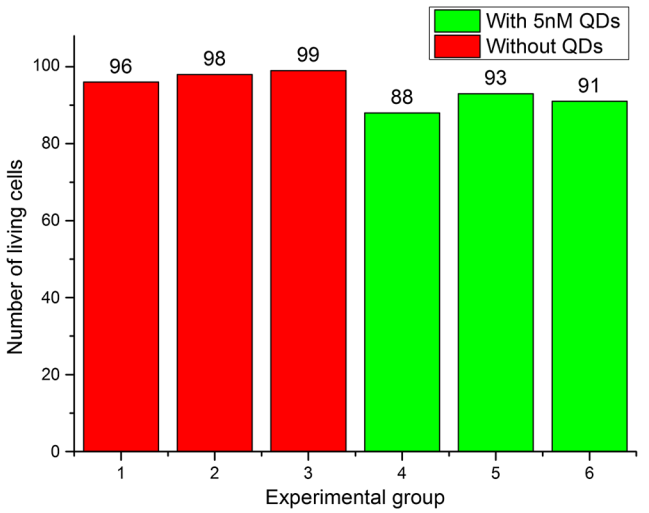

Fig. 11 The image of living cells' rate after culturing HL60 with and without QDs for 24 h. Total cell number of every group: 100.

one antigen at the same time for a long time with external stimuli. This meets the requirement for multiplexed detection of single-cell array.

3.7 *Potential Toxicity Associated with QDs*

To test QDs' cytotoxicity to HL60, we added 0.5 pmol QDs in an experimental group at 100 μL/well and cultured it for 24 h, which is the same as the QDs' concentration and tracing time in the multiplexed staining and detecting experiments above. Meanwhile, the control groups were cells of the same concentration at 100 μL/well without QDs. First, by comparing the appearance and the outline of experimental and control groups, we found no obvious difference. Second, we utilized Trypan Blue to test cells' survival rate. Survival rate = (1 − number of cell died/total number of cells) × 100%. The survival rate of control groups was 97.7%, and the survival rate of experimental groups was 90.7% (Fig. 11). Third, we utilized MTT kit to test QDs' inhibition to cell viability. Inhibition rate = [1 − (absorbance value of experimental groups − absorbance value of the blank)/(absorbance value of control groups − absorbance value of blank)] × 100%. To eliminate QDs' disturbance to the absorbance value, we added 0.5 pmol QDs in a control group just before testing it with microplate absorbance reader. The inhibition rate of QDs was 11.6% (Fig. 12). Therefore, by comparing cells' outline, survival rate, and testing inhibition rate, we found that QDs have some cytotoxicity to HL60, but the cytotoxicity was insignificant in 24 h and would not affect the experimental results of multiplexed staining and detection.

4 Conclusion

For cellular proteins optical tracing and imaging, we developed an easy, environmentally friendly, and low-cost way to prepare QDs of wide emitting fluorescence spectra ranging from purple to red. By controlling the ratio of Cd to Se, we achieved preparation of multiplexed QDs at low temperature within a shorter time period, that is safer, simpler, and more convenient than traditional methods.

We also used TGA to realize water-soluble modification for QDs. It is an easy method to modify QDs without changing the size and the characteristics of the QDs. This reduces the influence of water-soluble modification during cell labeling. TGA modification makes it full of carboxyl residues on the surface of QDs, which makes it easy to conjugate QDs to antibodies by forming amide bonds.

Finally, we showed multiplexed labeling of cells using different QDs by binding antibodies conjugated to QDs and antigens on the surface of the cells. Multiplexed staining is important, because we can obtain the relative quantity of antigens on the cells' surface by analyzing the mixed fluorescence of the cells. This method allows us to analyze changes in the quantity of antigens or proteins in a single cell in real time. Also, we can detect the influence of drugs or other environmental stimuli to cell receptors' expression and binding abilities between receptors and ligands or antagonists, offering effective methods to drug screening.

The approaches presented in this article for multiplexed living cells staining with QD bioprobes are applicable to optical cell sensors and instruments. With the same method, we can also label other targets (such as protein, peptides, biotinylated materials, and chemicals with amidogen) to study cells' behaviors. In further studies, we will utilize these bioprobes in the single-cell array to indicate the relative quantity of antigens and receptors expressed by the same cell in drug screening.

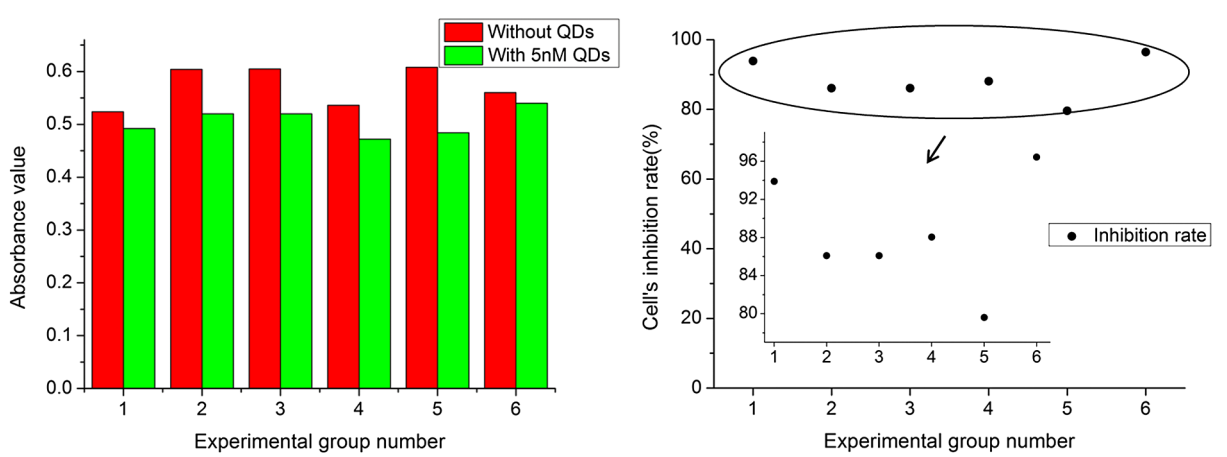

Fig. 12 The image of absorbance value after culturing HL60 with and without QDs for 24 h and inhibition rate of 5 nM QDs to HL60. Absorbance value = absorbance value of experimental groups (or control groups) – absorbance value of the blank.

Acknowledgments

This work is supported by the National Natural Science Foundation of China (No. 61071002), National Program for Significant Scientific Instruments Development of China (No. 2011YQ030134), the Funds for State Key Laboratory of China, and the Scientific Research Foundation for Returned Overseas Chinese Scholars. We also thank Professor Yinye Wang of Beijing University for the cell supports.

References

1. M. Y. Han et al., "Quantum-dot-tagged microbeads for multiplexed optical coding of biomolecules," *Nat. Biotechnol.* **19**(7), 631–635 (2001).
2. X. Michalet et al., "Quantum dots for live cells, in vivo imaging, and diagnostics," *Science* **307**(5709), 538–544 (2005).
3. C. Bullen and P. Mulvaney, "The effects of chemisorption on the luminescence of CdSe quantum dots," *Langmuir* **22**(7), 3007–3013 (2006).
4. R. Wargnier et al., "Energy transfer in aqueous solutions of oppositely charged CdSe/ZnS core/shell quantum dots and in quantum dot-nano-gold assemblies," *Nano Lett.* **4**(3), 451–457 (2004).
5. F. Q. Chen and D. Gerion, "Fluorescent CdSe/ZnS nanocrystal−peptide conjugates for long-term, nontoxic imaging and nuclear targeting in living cells," *Nano Lett.* **4**(10), 1827–1832 (2004).
6. M. Geszke et al., "Folic acid-conjugated core/shell ZnS:Mn/ZnS quantum dots as targeted probes for two photon fluorescence imaging of cancer cells," *Acta Biomater.* **7**(3), 1327–1338 (2011).
7. B. Dubertret et al., "In vivo imaging of quantum dots encapsulated in phospholipid micelles," *Science* **298**(5599), 1759–1762 (2002).
8. R. Yang, H. Yang, and L. W. Lin, "Quantum dot nano thermometers reveal heterogeneous local thermogenesis in living cells," *ACS Nano* **5**(6), 5067–5071 (2011).
9. C. Earhart et al., "Synthesis of carbohydrate-conjugated nanoparticles and quantum dots," *Langmuir* **24**(12), 6215–6219 (2008).
10. L. F. Qi and X. H. Gao, "Quantum dot–amphipol nanocomplex for intracellular delivery and real-time imaging of siRNA," *ACS Nano* **2**(7), 1403–1410 (2008).
11. T. H. Tian et al., "The origins of cancer robustness and evolvability," *Integr. Biol.* **3**(1), 17–30 (2011).
12. J. Foo and F. Michor, "Evolution of resistance to targeted anti-cancer therapies during continuous and pulsed administration strategies," *PLoS Comput. Biol.* **5**(11), e1000557 (2009).
13. S. M. Stuczynski, J. G. Brennan, and M. L. Steigerwald, "Formation of metal-chalcogen bonds by the reaction of metal-alkyls with silyl chalcogenides," *Inorg. Chem.* **28**(25), 4431–4432 (1989).
14. C. B. Murray, D. J. Norris, and M. G. Bawendi, "Synthesis and characterization of nearly monodisperse CdE (E = sulfur, selenium, tellurium) semiconductor nanocrystallites," *J. Am. Chem. Soc.* **115**(19), 8706–8715 (1993).
15. K. J. E. Bowen, V. L. Colvin, and A. P. Alivisatos, "X-ray photoelectron spectroscopy of CdSe nanocrystals with applications to studies of the nanocrystal surface," *J. Phys. Chem.* **98**(15), 4109–4117 (1994).
16. X. G. Peng, J. Wickham, and A. P. Alivisatos, "Kinetics of II-VI and III-V colloidal semiconductor nanocrystal growth: 'focusing' of size distributions," *J. Phys. Chem.* **120**(21), 5343–5344 (1998).
17. X. G. Peng et al., "Shape control of CdSe nanocrystals," *Nature* **404**, 59–61 (2000).
18. Z. A. Peng and X. G. Peng, "Formation of high-quality CdTe, CdSe, and CdS nanocrystals using CdO as precursor," *J. Am. Chem. Soc.* **123**(1), 183–184 (2001).
19. Z. T. Deng et al., "A new route to zinc-blende CdSe nanocrystals: mechanism and synthesis," *J. Phys. Chem. B* **109**(35), 16671–16675 (2005).
20. R. D. K. Misra, "Quantum dots for tumor targeted drug delivery and cell imaging," *Nanomedicine* **3**(3), 271–274 (2008).
21. P. Zhang and W. G. Liu, "ZnO QD@PMAA-co-PDMAEMA nonviral vector for plasmid DNA delivery and bioimaging," *Biomaterials* **31**(11), 3087–3094 (2010).
22. Y. L. Liu et al., "Fluorescence-enhanced gadolinium-doped zinc oxide quantum dots for magnetic resonance and fluorescence imaging," *Biomaterials* **32**(4), 1185–1192 (2011).
23. Q. Yuan, S. Hein, and R. D. K. Misra, "New generation of chitosan encapsulated ZnO quantum dots with drug: synthesis, characterization, and in-vitro drug delivery response," *Acta Biomater.* **6**(7), 2732–2739 (2010).
24. Z. Jia and R. D. K. Misra, "Tunable ZnO quantum dots for bioimaging: synthesis and photoluminescence," *Adv. Performance Mater.* **28**, 1–2 (2013).
25. W. C. W. Chan and S. M. Nie, "Quantum dot bioconjugates for ultra-sensitive nonisotopic detection," *Science* **281**(5385), 2016–2018 (1998).
26. S. Pathak et al., "Hydroxylated quantum dots as luminescent probes for in situ hybridization," *J. Am. Chem. Soc.* **123**(17), 4103–4104 (2001).
27. Y. F. Chen and Z. Rosenzweig, "Luminescent CdSe quantum dot doped stabilized micelles," *Nano Lett.* **2**(11), 1299–1302 (2002).
28. C. Earhart et al., "Synthesis of carbohydrate-conjugated nanoparticles and quantum dots," *Langmuir* **24**(12), 6215–6219 (2008).
29. X. Gao et al., "In vivo cancer targeting and imaging with semiconductor quantum dots," *Nat. Biotechnol.* **22**, 969–976 (2004).
30. N. Insin et al., "Incorporation of iron oxide nanoparticles and quantum dots into silica microspheres," *ACS Nano* **2**(2), 197–202 (2008).
31. Z. B. Lin et al., "Studies on quantum dots synthesized in aqueous solution for biological labeling via electrostatic interaction," *Anal. Biochem.* **319**(2), 239–243 (2003).
32. N. Li and C. M. Ho, "Photolithographic patterning of organosilane monolayer for generating large area two-dimensional B lymphocyte arrays," *Lab Chip* **8**, 2105–2122 (2008).
33. D. H. Ren et al. "A single cells patterning approach for human promyelocytic leukemia cells," in *3rd Int. Conf. CSMNT*, Hangzhou, China (2012).
34. D. Brackman, F. Lund-Johansen, and D. Aarskog, "Expression of leukocyte differentiation antigens during the differentiation of HL-60 cells induced by 1,25-dihydroxyvitamin D3: comparison with the maturation of normal monocytic and granulocytic bone marrow cells," *J. Leukocyte Biol.* **58**(5), 547–555 (1995).
35. C. Y. Hsu and B. Y. M. Yung, "Over-expression of nucleophosmin/B23 decreases the susceptibility of human leukemia HL-60 cells to retinoic acid-induced differentiation and apoptosis," *Int. J. Cancer* **88**(3), 392–400 (2000).
36. R. K. Zhong et al., "Cytotoxicity of anti-CD64-ricin a chain immunotoxin against human acute myeloid leukemia cells in vitro and in SCID mice," *J. Hematother. Stem Cell Res.* **10**(1), 95–105 (2001).
37. C. Friesen et al., "Breaking chemoresistance and radioresistance with [213Bi]anti-CD45 antibodies in leukemia cells," *Cancer Res.* **67**(5), 1950–1958 (2007).
38. Q. Wang et al., "Luminescent properties of water-soluble denatured bovine serum albumin-coated CdTe quantum dots," *J. Phys. Chem. B* **110**(34), 16860–16866 (2006).
39. W. C. W. Chan and S. M. Nie, "Quantum dot bioconjugates for ultra-sensitive nonisotopic detection," *Science* **281**(5385), 2016–2018 (1998).